JOURNAL OF VIROLOGY, Aug. 2003, p. 8524–8531 Vol. 77, No. 15
0022-538X/03/$08.00+0 DOI: 10.1128/JVI.77.15.8524–8531.2003

Human Cellular Nucleic Acid-Binding Protein Zn^{2+} Fingers Support Replication of Human Immunodeficiency Virus Type 1 When They Are Substituted in the Nucleocapsid Protein

Connor F. McGrath,[1] James S. Buckman,[2] Tracy D. Gagliardi,[2] William J. Bosche,[2] Lori V. Coren,[2] and Robert J. Gorelick[2]*

Developmental Therapeutics Program—Target Structure Based Drug Discovery Group[1] and AIDS Vaccine Program, Science Applications International Corporation—Frederick, Inc.,[2] National Cancer Institute at Frederick, Frederick, Maryland 21702-1201

Received 16 December 2002/Accepted 8 May 2003

A family of cellular nucleic acid binding proteins (CNBPs) contains seven Zn^{2+} fingers that have many of the structural characteristics found in retroviral nucleocapsid (NC) Zn^{2+} fingers. The sequence of the NH_2-terminal NC Zn^{2+} finger of the pNL4-3 clone of human immunodeficiency virus type 1 (HIV-1) was replaced individually with sequences from each of the seven fingers from human CNBP. Six of the mutants were normal with respect to protein composition and processing, full-length genomic RNA content, and infectivity. One of the mutants, containing the fifth CNBP Zn^{2+} finger (CNBP-5) packaged reduced levels of genomic RNA and was defective in infectivity. There appear to be defects in reverse transcription in the CNBP-5 infections. Models of Zn^{2+} fingers were constructed by using computational methods based on available structural data, and atom-atom interactions were determined by the hydropathic orthogonal dynamic analysis of the protein method. Defects in the CNBP-5 mutant could possibly be explained, in part, by restrictions of a set of required atom-atom interactions in the CNBP-5 Zn^{2+} finger compared to mutant and wild-type Zn^{2+} fingers in NC that support replication. The present study shows that six of seven of the Zn^{2+} fingers from the CNBP protein can be used as substitutes for the Zn^{2+} finger in the NH_2-terminal position of HIV-1 NC. This has obvious implications in antiviral therapeutics and DNA vaccines employing NC Zn^{2+} finger mutants.

Retroviral nucleocapsid (NC) and its Zn^{2+} fingers are found to be critical for many steps in the viral life cycle. Studies have shown NC's involvement in virion assembly (5, 10, 15, 17–19, 49), reverse transcription (7, 24, 46, 51), and even integration processes (7–9). The Zn^{2+} finger in NC is one of the most highly conserved elements (4, 11) in the orthoretroviruses (52). NC, as a domain of the Gag precursor, is involved in the assembly of virions and packaging of the genomic RNA. The NC protein, generated during maturation of virions through the action of the viral protease, is involved in the reverse transcription and integration steps of the virus life cycle. The Zn^{2+} finger structures are critical for the survival of retroviruses, since this and other laboratories have shown that a variety of alterations to the Zn^{2+} fingers typically result in particles that are replication defective (14, 20, 25, 26, 51). When the Cys or His residues are changed to amino acids that no longer bind Zn^{2+}, virions are defective in RNA packaging and replication. Thus, the highly conserved NC Zn^{2+} finger structures are critical for assembly and infection processes.

It was observed that a number of NC mutant murine leukemia and human immunodeficiency virus type 1 (HIV-1) viruses were still able to package their RNA genomes, and yet they were replication defective (20, 22, 25). NC in these mutants is still able to coordinate significant levels of Zn^{2+} since the metal-coordinating residues are substituted with other Zn^{2+} coordinating amino acids (36). The replication defects in these mutants manifest themselves at the level of reverse transcription, since there is a reduction in the level of viral DNA (vDNA) produced upon infection. There is also a major defect in the ability of the these NC mutant virions to protect their vDNA once it is generated (7, 24, 51). In one particular HIV-1 NC mutant (NC_{H23C}), there is also a defect in the ability of virions to mediate the end processing of the vDNA prior to integration, suggesting that NC and its Zn^{2+} fingers function in the preintegration with the viral integrase protein (7). Thus, one can observe the central importance of NC and the conserved Zn^{2+} finger structures at various critical stages of the viral life cycle.

Surprisingly, there is a class of proteins called cellular nucleic acid binding proteins (CNBPs) that contain seven Zn^{2+} finger sequences that are very similar to those found in retroviral NC (3, 6, 12, 35, 45, 47, 55). Retroviral NC and CNBP Zn^{2+} fingers have arrangements of amino acids with the general sequence: "–Cys–ϕ–X–Cys–Gly–±–X–Gly–His–X_3–δ–Cys–," where X is a variable amino acid, ϕ is an aromatic residue, "±" is a charged amino acid, and δ is a carbonyl-containing residue. There is absolute amino acid homology between retroviral NC and CNBP Zn^{2+} fingers among the Cys and His metal ion-binding residues (CCHC) and the two Gly residues listed above. Additionally, there is conservation of the positions of functionally homologous residues within the Zn^{2+} finger loops with an aromatic residue (ϕ) in the first loop, a charged residue (±) in the second loop, and a carbonyl-containing amino acid (δ) in the third loop (Table 1). CNBPs from

* Corresponding author. Mailing address: AIDS Vaccine Program, Science Applications International Corporation—Frederick, Inc., National Cancer Institute at Frederick, Frederick, MD 21702-1201. Phone: (301) 846-5980. Fax: (301) 846-7119. E-mail: gorelick@ncifcrf.gov.

TABLE 1. Comparison of the HIV-1 NC Zn^{2+} fingers with the seven Zn^{2+} fingers from human CNBP

Zn^{2+} finger	Amino acid[a] at position:													
	1	2	3	4	5	6	7	8	9	10	11	12	13	14
HIV-1 NH_2 terminus	Cys	Phe	Asn	Cys	Gly	Lys	Glu	Gly	His	Ile	Ala	Lys	Asn	Cys
CNBP-1[b]	–	–	Lys	–	–	Arg	Ser	–	–	Trp	–	Arg	Glu	–
CNBP-2	–	Tyr	Arg	–	–	Glu	Ser	–	–	Leu	–	–	Asp	–
CNBP-3	–	Tyr	–	–	–	Arg	Gly	–	–	–	–	–	Asp	–
CNBP-4	–	Tyr	–	–	–	–	Pro	–	–	Leu	–	Arg	Asp	–
CNBP-5	–	Tyr	Ser	–	–	Glu	Phe	–	–	–	Gln	–	Asp	–
CNBP-6	–	Tyr	Arg	–	–	Glu	Thr	–	–	Val	–	Ile	–	–
CNBP-7	–	Tyr	Arg	–	–	Glu	Ser	–	–	Leu	–	Arg	Glu	–
HIV-1 COOH terminus	–	Trp	Lys	–	–	–	–	–	–	Gln	Met	–	Asp	–

[a] The positions of the first amino acids of the HIV-1 NH_2- and COOH-terminal NC Zn^{2+} fingers are 15 and 36, respectively. The positions of the first Cys residue in each of the seven human CNBP Zn^{2+} fingers are 6, 54, 74, 97, 119, 137, and 158 (45). A dash (–) indicates that the amino acid is the same as that found in the HIV-1 NH_2-terminal NC Zn^{2+} finger.

[b] The number after CNBP refers to the order of the Zn^{2+} finger from the NH_2 terminus out of a total of seven Zn^{2+} fingers.

a number of vertebrates are highly homologous at the protein and nucleic acid levels. They have been found in humans (45), rodents (6, 35, 55), chickens (47), and amphibians (3, 12).

The true functions of CNBPs among the various species listed are still under study. Initial reports on mammalian CNBP indicate that it binds to the sterol response element (SRE) (42, 45, 54), which regulates cholesterol levels. Later studies suggested that CNBP was probably not involved in sterol regulation (41, 55, 56). In rodents, CNBP was found to enhance promoter activity of the colony-stimulating factor 1 promoter upon binding (35). A cDNA coding for CNBP has been generated from the mRNA isolated from a wide array of tissues in chickens (47). CNBP was shown to be a translational regulatory factor for ribosomal proteins and is differentially expressed at various stages of development in amphibians (3, 12, 43). Another CNBP was found to interact with JC virus promoter-enhancers (39). There has recently been a report of another human protein that has Zn^{2+} fingers with most of the characteristics of the retroviral NC Zn^{2+} finger, which is related to the Mpe1p protein found in yeast (53).

As the CNBP and retroviral NC Zn^{2+} fingers generally appear to function in nucleic acid interactions in their respective systems and have quite similar sequences, we wished to determine whether CNBP Zn^{2+} fingers could serve as suitable substitutes for the proximal NC Zn^{2+} finger in HIV-1 NC. In the present study, the seven Zn^{2+} fingers from human CNBP were individually exchanged into HIV-1 NC, and mutant viruses were characterized. An analysis was also performed to model the Zn^{2+} finger structures from CNBP and HIV-1 NC in an attempt to identify possible divergent structural features, which may partially explain why one of the mutants was replication defective.

MATERIALS AND METHODS

Cell lines. The H9 (44) 293T (293 cell line containing the simian virus 40 large T antigen [22]), and the HCLZ (CD4-producing HeLa cells containing an HIV-1 long terminal repeat [LTR]–β-galactosidase construct [23]) cell lines were described previously. The H9 and HCLZ cell lines were cultured in the presence of hexadimethrine bromide (Polybrene [Sigma-Aldrich, St. Louis, Mo.] at 2 μg/ml). All lines were maintained in 7% CO_2 at 37°C unless otherwise noted.

Mutagenesis. Primers were obtained from either the DNA Support Laboratory to the National Cancer Institute at Frederick, Science Applications International Corporation—Frederick, Inc., Frederick, Md.; from Operon Technologies, Inc. (Alameda, Calif.); or Invitrogen (Carlsbad, Calif.). Restriction enzymes and T4 DNA ligase were from Invitrogen or New England BioLabs, Inc. (Beverly, Mass.).

Mutations were introduced by PCR using a Perkin-Elmer PE9600 thermocycler and Applied Biosystems AmpliTaq core reagents (Foster City, Calif.) according to the manufacturer's instructions. Sequences used for the CNBP Zn^{2+} finger substitutions were obtained from that reported by Rajavashisth and coworkers (45) (GenBank accession number M28372). The sense and antisense primers contain *Spe*I and *Apa*I sites, respectively (that correspond to sites at bp 1507 and 2006, respectively, in pNL4-3), which were used for subsequent cloning of the PCR products into pNL4-3 (GenBank accession number AF324493 [1]). pDR0 (23) was used as the DNA source for the PCR. The PCR fragments were reintroduced into pDR0 and then the mutant pDR0 plasmids and pNL3-4 were digested with *Spe*I and *Sal*I. The appropriate fragments were isolated by agarose gel electrophoresis and then ligated, yielding the full-length pNL4-3-based proviral plasmid clones designated pCNBP-1 through pCNBP-7.

Virus characterization. Exogenous template reverse transcriptase (RT) assays were performed on clarified supernatants as described previously (7, 27). Immunoblot analysis was performed as described previously (25, 27). Viral $p24^{CA}$ antigen levels were determined by using the reagents and procedures for the AVP, Biological Products Laboratory's (National Cancer Institute at Frederick, Frederick, Md.) HIV-1 p24 enzyme-linked immunosorbent assay (ELISA) kit. RNA was isolated as described previously (18, 25). HIV-1 RNA blot analysis was performed as described previously (27); however, instead of examining blots by autoradiography, phosphorimager analysis was performed with a Bio-Rad (Hercules, Calif.) Molecular Imager FX instrument. Long-term and single-round infectivity analyses of NC mutant and wild-type viruses were performed with clarified samples from transfected 293T cells by limiting dilution with H9 and HCLZ cells, respectively, as described previously (23, 25, 27). vDNA was prepared from infected cells, and quantitative PCR analysis was performed to detect the R/U5, U3/U5, *gag*, and R/5′-untranslated region target sequences as described previously (7).

Computational modeling. To note any obvious differences in Zn^{2+} finger structures and to attempt to find additional correlates of why one of the HIV-1 NC mutants was defective in replication and RNA packaging (see below), comparisons were performed on structural models of a number of CNBP and the NH_2-terminal HIV-1 NC Zn^{2+} fingers. Molecular dynamics, hydropathic analysis (31, 34), and classical factor analysis techniques (30, 38, 48) were used, and the collective techniques are referred to as "hydropathic orthogonal dynamic analysis of protein" (HODAP). Published coordinates for the NH_2-terminal HIV-1 NC Zn^{2+} finger (50) were used to homology model (Accelrys; Insight 2000 Molecular Modeling Workbench, San Diego, Calif.) the CNBP-3 and CNBP-5 structures. Identical amino acid residues in the CNBP model structures were directly superimposed on the HIV template structure, and nonidentical residues were placed with the side chain maximally overlapping the template side chain. This set of three starting structures was subjected to a protocol of molecular dynamics calculations. Individual geometries were samples from the trajectory at 1-ps intervals for 200 ps.

The HINT intramolecular hydropathic potential function (31, 34), which measures atom-atom interactions in terms of four hydropathic interaction categories, was utilized. This methodology reduces the empirical information from bulk molecular solvent partitioning to discrete atom-atom interactions. Because of this approach, the hydrophobic constants derived include a linear-free estimate

TABLE 2. RT and $p24^{CA}$ properties of NC mutant and wild-type HIV-1

Mutant[a]	RT (cpm/ml)[b]	Mean $p24^{CA}$ (ng/ml)[c] level ± SD
(−)-Control[d]	0	0
CNBP-1	$(4.0 \pm 1.0) \times 10^6$	220 ± 50
CNBP-2	$(2.1 \pm 0.1) \times 10^6$	100 ± 10
CNBP-3	$(2.8 \pm 0.9) \times 10^6$	130 ± 10
CNBP-4	$(1.9 \pm 0.2) \times 10^6$	140 ± 10
CNBP-5	$(1.9 \pm 0.4) \times 10^6$	100 ± 30
CNBP-6	$(1.8 \pm 0.1) \times 10^6$	40 ± 20
CNBP-7	$(2.3 \pm 0.3) \times 10^6$	40 ± 20
Wild-type HIV-1	$(2.3 \pm 0.2) \times 10^6$	50 ± 30

[a] Mutants are described in Table 1.
[b] Counts per minute of [^{3}H]TMP incorporated per milliliter of culture fluid. Values represent the average of two replicates from a single harvest.
[c] Determined by $p24^{CA}$ antigen ELISA from the AIDS Vaccine Program, Biological Products Laboratory. Values represent the average of five replicates from a single harvest.
[d] (−)-Control is from cultured cells transfected with sheared salmon sperm DNA.

of entropy, which is ignored in most molecular mechanics models. Unfavorable interactions consist of hydrophobic-polar and base-base pairs, while the favorable interactions consist of hydrophobic-hydrophobic and acid-base pairs. Hydrogen bonds fall under the category of acid-base interactions in this scheme. This method has been used successfully in a number of structure activity surveys (2, 28, 29, 31–33, 40). Two hundred frames from each of the dynamic trajectories were analyzed by using HINT, which produced a trajectory data set in 14 dimensions, one for each of the residues in each of the model Zn^{2+} finger peptides studied. This data set contains geometric information in the form of the distance-dependent N^2 interactions and hydropathic information. Salient patterns of variation were extracted from this data set by using factor analysis (30, 38, 48) and examined in light of the phenotypic data available for the particular Zn^{2+} finger. The resulting set of factor loading coefficients could be interpreted as measures of the unique contribution made by each factor to the variance of the original variables.

The original HINT data set for a single Zn^{2+} finger trajectory consists of over 67,000 lines of specific atom-atom interactions. Identifying amino acids with high factor loadings as indicated by the factor analysis provides a basis for filtering this large data set to permit a more detailed examination of predominant interactions between amino acids. Used in combination with animated playbacks of the trajectory, these techniques allow for the rapid elimination of all but the most persistent amino acid interactions in the model systems.

RESULTS

Analysis of viral proteins. To determine whether the Zn^{2+} fingers from the human CNBP protein could function in HIV-1 NC, DNA plasmids that contained the various NH_2-terminal NC Zn^{2+} finger sequences shown in Table 1 were constructed. The mutant proviral constructs, pCNBP-1 through pCNBP-7 and pNL4-3, were transfected, and viruses were obtained and analyzed. To determine the quantity of viruses produced from the transfections, RT activities and $p24^{CA}$ levels from supernatants, harvested 48 h posttransfection, are presented in Table 2 from a typical transfection. There was some variation among the same samples obtained from different transfections due to variations in transfection efficiencies but, overall, the mutants have RT and $p24^{CA}$ levels that are similar to the wild-type virus within a transfection experiment.

To examine the state and relative levels of the various proteins contained in the virions, immunoblot analyses were performed on pelleted virus obtained from the transfections. Figure 1 presents an immunoblot of mutant and wild-type HIV-1 where samples were adjusted for equivalent levels of RT activity. Antisera that detect $p7^{NC}$, $p24^{CA}$, and $gp120^{SU}$ were used to sequentially identify NC, CA, and SU containing viral proteins. All of the mutants express viral Env and Gag proteins at levels similar to those found in wild-type HIV-1. Processing of the Gag polyproteins in most of the mutants is also similar to that found in the wild-type sample. Note that the levels of processed $p24^{CA}$ in the mutants are nearly identical to those found in the wild-type sample in the $p24^{CA}$ blot, indicating that the Gag/Gag-Pol ratios are similar among all of the viruses. In all of the immunoblots examined, it was observed that CNBP-5 contained a bit more partially processed $Pr55^{Gag}$ than the other mutant and wild-type viruses. In addition, a darker band for the CNBP-4 sample in the $p7^{NC}$ blot was always observed. This is probably due to a higher avidity of $p7^{NC}$ antibodies for the CNBP-4 Zn^{2+} finger mutant containing $p7^{NC}$ and $Pr55^{Gag}$ proteins. The $p7^{NC}$ antiserum detects the other NC-containing proteins with slightly varying intensities, even though the $p24^{CA}$ intensities were nearly identical.

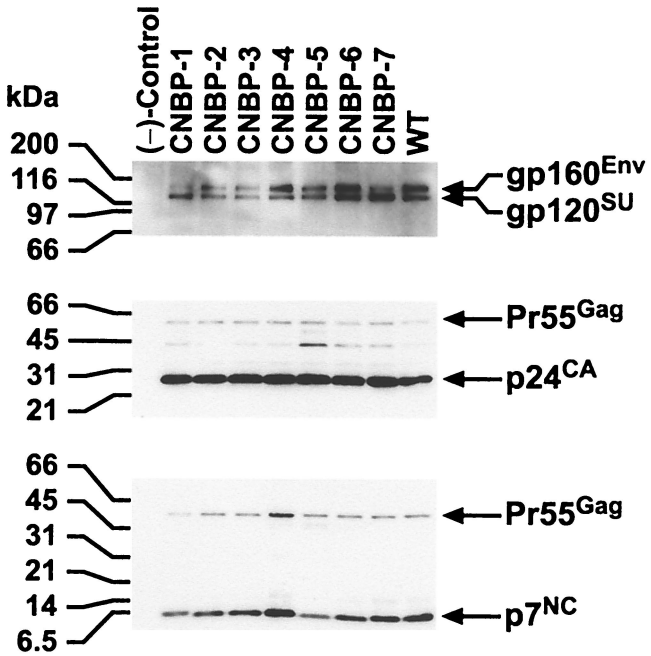

FIG. 1. Immunoblot analysis of NC mutant and wild-type HIV-1. Proteins were fractionated by sodium dodecyl sulfate-polyacrylamide gel electrophoresis and transferred to an Immobilon-P (Millipore) membrane. A total of 6.1×10^6 cpm of RT activity/ml for each sample was loaded onto the gel. The membrane was incubated sequentially with α-$p7^{NC}$ (bottom panel), α-$p24^{CA}$ (middle panel), and α-$gp120^{SU}$ (top panel). Bands were detected by chemiluminescence as described previously (25, 27). Molecular weight markers are indicated on the left, the virus analyzed is designated at the top, and the pertinent proteins detected by the various antibodies are specified on the right.

Analysis of viral RNA. The full-length viral RNA content of these viruses was examined and compared to wild-type HIV-1 to determine the RNA packaging efficiencies of the mutants. Figure 2A shows an RNA blot of virus samples obtained from a typical transfection; the samples were again adjusted for equivalent RT levels. Most of the mutants, except for CNBP-5, contain significant levels of full-length viral RNA. Phosphorimager analysis was performed on three Northern blots, the

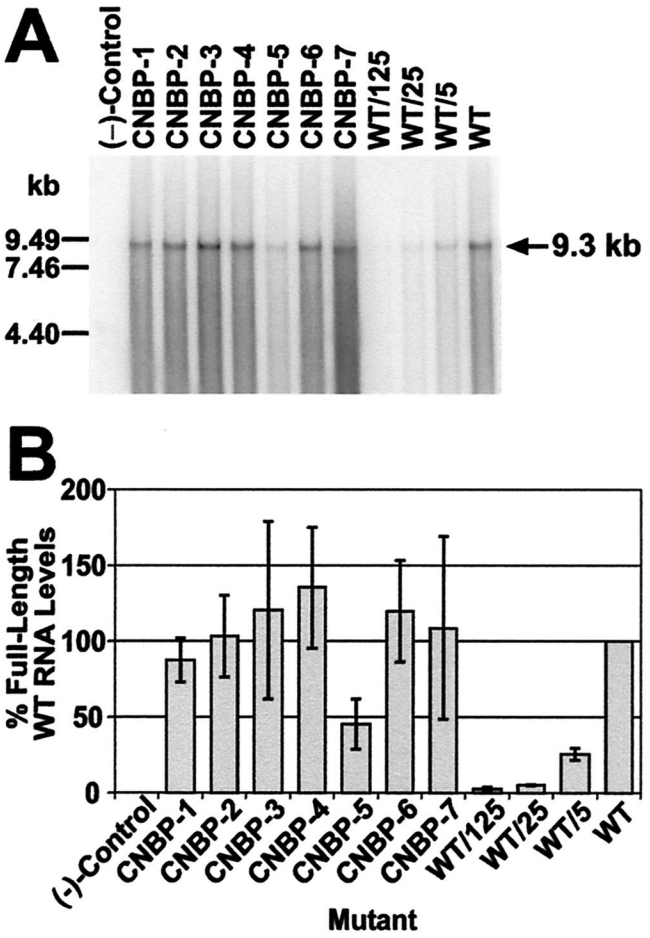

FIG. 2. Hybridized RNA blot and phosphorimager analysis of NC mutant and wild-type HIV-1 transiently expressed in 293T cells. (A) Particles were analyzed for full-length HIV-1 genomic RNA by using a ^{32}P-labeled probe comprised of an 8.1-kbp *Ava*I pNL4-3 fragment. All samples were adjusted for equal RT levels (4.1×10^6 cpm), fractionated, and treated as described in Materials and Methods. Dilutions (undiluted, 5-, 25-, and 125-fold) of the wild-type sample were also tested. (−)-Control, samples isolated and prepared from centrifuged supernatants from 293T cells transfected with sheared salmon sperm DNA. The RNA markers are indicated on the left and the size of full-length HIV-1 RNA genome is noted on the right. (B) Band intensities were obtained by phosphorimager analysis from Northern blots (performed as described in Materials and Methods and in part A of this figure) from three independent transfections. The samples for each Northern blot were adjusted for equal levels of RT activity. The intensity of the undiluted wild-type sample (WT) was set to 100% and the intensities of the remaining samples and dilutions of the wild-type sample were calculated relative to the undiluted wild-type sample. The percentage of full-length wild-type RNA levels obtained is representative of the average of three independent RNA blots. Error bars depicting the standard deviation from the mean are also presented. (−)-Control is as described for panel A.

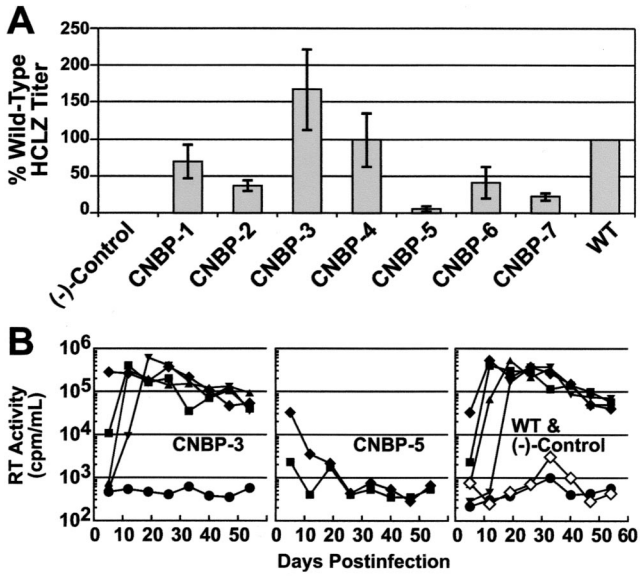

FIG. 3. Infectivity analysis of NC mutant and wild-type HIV-1 samples. (A) Single-round infectivity titers were obtained by infecting HCLZ cells as described in Materials and Methods and corrected for a constant level of RT activity within an assay series. The titer levels of the mutants are reported as the percentage of the wild-type sample for a particular assay series with the wild-type sample (WT) set to 100%. The percentage of wild-type HCLZ titers presented is representative of the average infectivity of samples from four independent transfections. Error bars, indicating the standard deviation from the mean, are also presented. (−)-Control samples are from 293T cells transfected with sheared salmon sperm DNA. (B) Long-term H9 replication assays of NC mutant and wild-type HIV-1 viruses are presented. RT activities of the starting inoculum, corrected for background (in counts per minute of [^{3}H]TMP incorporated/ml) are as follows: (CNBP-3), 2.1×10^6; (CNBP-5), 1.8×10^6; and (wild-type), 0.4×10^6. Symbols: ◆, undiluted; ■, 1/20; ▲, 1/400; ▼, 1/8,000; ●, 1/160,000; ◇, (−)-Control (supernatants from 293T cells transfected with sheared salmon sperm DNA).

samples of which were obtained from three independent transfections. The percentage of wild-type levels of full-length viral RNA in the mutants were calculated for each blot, and the average RNA content of the mutants are presented in Fig. 2B. All of the mutants except CNBP-5 contain >85% wild-type levels of full-length viral RNA. CNBP-5 contains <50% wild-type levels of RNA genomes. The analyses thus far indicate that the characteristics of CNBP-5 deviate from those of the other mutant and wild-type viruses.

Infectivity analyses of viruses. To assess how the CNBP Zn^{2+} finger substitutions affected virion infectivity and replication, assays were next performed with the mutant and wild-type viruses by using single-round infection and long-term culture assays. Supernatants from transfections were applied to HCLZ cells to determine whether the virions could make sufficient Tat protein to activate the LTR–β-galactosidase reporter gene. Four independent transfections were performed and tested with the HCLZ cells. Figure 3A shows that the CNBP-1, -3, and -4 mutants have single-round infectivity titers near wild-type levels (>50% of the wild-type titer). The CNBP-2, -6, and -7 mutants have titers that are less than half of the wild-type HCLZ titer. CNBP-5 demonstrated the most drastic reduction in its titer, which was ~5% that of wild-type.

Long-term infectivity analyses were also performed on mutant and wild-type samples to examine the ability of these viruses to replicate in H9 cells. Four to five independent transfections were performed on each mutant and wild-type sample, and virus-containing supernatants were tested on the H9 cells. Results are presented in Fig. 3B, and all of the mutants replicate at levels similar to the wild-type virus, except for CNBP-5;

TABLE 3. Reverse transcription intermediate levels from mutant and wild-type virus infections

Virus	Mean level ± SD[a] of:			
	SS	FST	Gag	SST
(−)-Control[b]	0.0	0.0	0.0	0.0
CNBP-3	1.2 ± 0.1	1.3 ± 0.3	1.4 ± 0.3	1.1 ± 0.2
CNBP-5	0.05 ± 0.01	0.04 ± 0.01	0.03 ± 0.01	0.04 ± 0.01
Wild type	1.0	1.0	1.0	1.0

[a] Values are reported for each reverse transcription intermediate relative to values obtained from the wild-type virus. The average of two independent transfection-infection experiments is presented. SS is the minus-strand strong-stop DNA, the R/U5 target sequence (7). FST is first-strand transfer vDNA, the U3/U5 target sequence. Gag is the *gag* target sequence. SST is second-strand transfer vDNA, the R/5′-untranslated region target sequence.

[b] Mock infection was done with clarified sheared salmon sperm DNA transfection supernatants.

the CNBP-3 mutant is presented as a representative example of one of the replication-competent mutants. The CNBP-5 mutant was consistently replication-defective, even when tested undiluted (<1 tissue culture infective dose/ml; Fig. 3B). Replication of all of the mutant and wild-type viruses (except for CNBP-5) initiated from the onset of the assay, as opposed to viruses that have retarded initial replication kinetics and then revert to a wild phenotype, such as the NC1/1 mutant reported previously (23). All of the replication-competent HIV-1 mutants were examined at the end of the H9 infectivity analyses; it was determined that the mutant genotypes were maintained throughout the 8-week culture period. This was determined by PCR amplifying and sequencing the NC genes from total DNA isolated from the infected cells, as described previously (25).

Quantitative PCR of reverse transcription intermediates. In an effort to determine mechanistically why the CNBP-5 mutant was replication defective in the infectivity assays, we analyzed reverse transcription products after 24 h of infection by using the quantitative PCR-based approach with the TaqMan system described by Buckman et al. (7). It is apparent from results presented in Table 3 (data obtained from two independent transfection-infection experiments) that substitution of the CNBP-3 sequence results in little, if any, difference from the wild-type, as expected. In contrast, the CNBP-5 substitution results in a reduction of all reverse transcription intermediates examined, to a similar extent. Only 4 to 5% wild-type levels of all of the intermediates were observed for CNBP-5.

Comparison of molecular models of CNBP and the NH_2-terminal HIV-1 NC Zn^{2+} fingers. In attempts to further understand at the structural level why the CNBP-5 NC mutant was replication defective, we compared molecular models of the CNBP-3, CNBP-5, and the retroviral NH_2-terminal NC Zn^{2+} fingers. The method employed here measures interactions within a Zn^{2+} finger and can point to pervasive atom-atom interaction differences between modeled structures that might account for the functional differences observed in the in vivo analyses. There are probably other protein-protein or protein-nucleic acid interactions that are altered when these mutations are introduced, although they are far too complex to analyze on a larger scale in this way. Nevertheless, this method has revealed its usefulness in identifying persistent interactions among the amino acid residues within loops among a single Zn^{2+} finger, and these interactions can be compared between different fingers.

Factor analysis reveals that the first five principal components of these data accounted for 50 to 60% of the variance in the HODAP data. Further examination of the first three components revealed some interesting features of the interactions within each Zn^{2+} finger trajectory, and residues identified by this method are listed below and shown in Fig. 4. Identification of the specific atom-atom interactions responsible for observed patterns was accomplished by filtering the raw data in accordance with the results of the HODAP.

The wild-type HIV-1 Zn^{2+} finger peptide trajectory recognized persistent hydrophobic interactions between the δ-carbons of Ile-10 and the ring carbons in Phe-2 (position numbering is as presented in Table 1). A similar pattern of hydrophobic interaction was observed between the Tyr-2 ring and the δ-carbons of Ile-10 in the CNBP-3 peptide trajectory. This indicates that the substitution of one aromatic residue for another (a Tyr for the Phe in this position) does not affect the persistent interaction of hydrophobic ring carbons with Ile-10 (Fig. 4A and B). It should be noted that previous in vivo results show that aromatic residue exchanges can be made and replication is still accommodated (14).

The interaction of hydrophobic ring carbons from the aromatic residue at position 2 with Ile-10 is absent in CNBP-5. Instead, an interaction between the Ser-3 hydroxyl group and the backbone oxygen of Tyr-2 dominates the HODAP pattern. Additionally, the Tyr-2 hydroxyl and the carboxyl group on Gln-11 remain in close proximity throughout the trajectory. Both of these interactions appear to occur at the expense of any hydrophobic interaction between the Ile-10 and Tyr-2 (Fig. 4C). The differences observed between CNBP-5 and the other Zn^{2+} finger models examined point to a possible structural explanation for the functional differences observed between the CNBP-5 mutant and the replication-competent viruses.

DISCUSSION

It is known that the highly conserved Zn^{2+} finger structures in retroviral NC are critical for assembly, reverse transcription, and integration processes (5, 7, 9, 10, 17, 24, 46, 51). It has been shown that even minor alterations to NC Zn^{2+} fingers are not tolerated and that virions are rendered replication defective. Therefore, it was quite surprising to find a group of retrovirus-like Zn^{2+} finger structures, with a wide array of substitutions (Table 1) that could support virus replication. There is conservation of the ligand-binding residues (Cys and His), as well as of the two glycine residues; thus, substitutions occur in the eight remaining amino acid positions. It is possible that the CNBP Zn^{2+} fingers in these proteins were somehow derived or related to retroviral NC Zn^{2+} fingers; they are amazingly similar to HIV-1 NC's Zn^{2+} fingers (see Table 1).

Surprisingly, the substitutions yielded structurally and functionally competent viruses. The only exception was the CNBP-5 Zn^{2+} finger mutant (Table 1). Previous observations suggested that retroviral NC Zn^{2+} fingers were quite sensitive to alteration, even when the positions of the NH_2- and COOH-terminal NC Zn^{2+} finger sequences are switched (23). All of the viruses except CNBP-5 appear normal with respect to protein content and processing (Table 2 and Fig. 1). CNBP-5

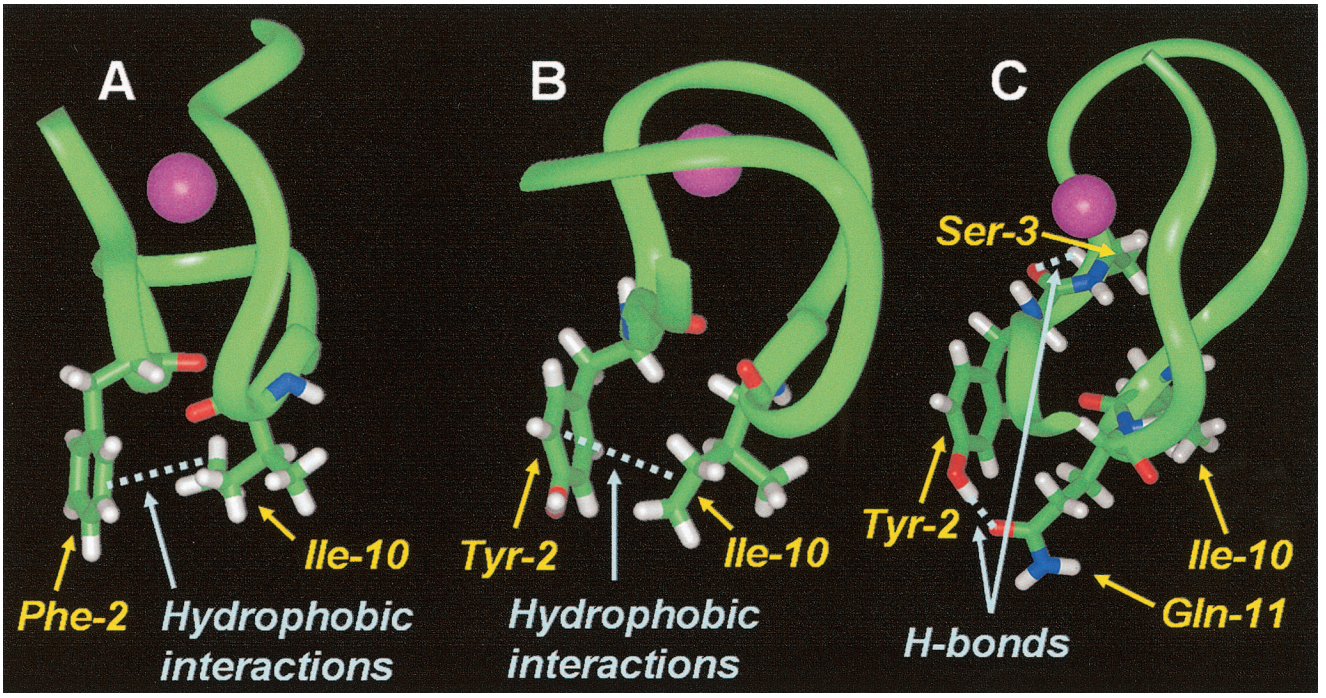

FIG. 4. Partial structures of mutant and wild-type Zn^{2+} fingers. Ribbon diagrams of the Zn^{2+} fingers are presented with the purple sphere representing the Zn^{2+} ion. Significant interactions are shown by the light-blue dashed lines. (A) The NH_2-terminal HIV-1 NC Zn^{2+} finger is shown with the persistent hydrophobic interactions between the δ-carbons of Ile-10 and the ring carbons in Phe-2. (B) The CNBP-3 Zn^{2+} finger is shown with similar hydrophobic interactions between the Tyr-2 ring and the Ile-10 δ-carbons. (C) The CNBP-5 Zn^{2+} finger shown has the indicated hydrogen bonds between the Ser-3 hydroxyl group and the backbone oxygen of Tyr-2, and the Tyr-2 hydroxyl and the carboxyl group on Gln-11, which have disrupted the hydrophobic interactions between the δ-carbons of Ile-10 and the ring carbons of Tyr-2.

particles have a slight defect shown by the accumulation of Gag-processing intermediates. The RNA content of most of the mutant viruses is similar to that of wild-type virus, with CNBP-5, again, being the outlier. CNBP-5 diverges from the other viruses with respect to infectivity as well. It is the most defective mutant in the single-round infection HCLZ assay (Fig. 3A), with only 5% of the titer found in the wild-type virus. Additionally, CNBP-5 is replication defective in a long-term infectivity assay when cultivated in H9 cells (Fig. 3B). Like HIV-1 NC, CNBP shows a preference for GT-rich sequences (16, 45). Perhaps the ability of many of the CNBP Zn^{2+} fingers to substitute faithfully for the NH_2-terminal Zn^{2+} finger in NC results from recognition of GT (U) sequences that are critical for NC binding during the viral life cycle (e.g., the stem-loop structures within the Ψ site and also at the LTR ends where protection of the full-length linear vDNA ends is critical for the subsequent integration process [7]).

The reverse transcription intermediate levels of cells infected with CNBP-5 were measured and compared to two replication-competent viruses (Table 3) by using techniques described previously (7). CNBP-5 clearly has a deficiency in its ability to synthesize vDNA upon infection. The defect in infectivity cannot be accounted for solely by the reduction in full-length genomic RNA as this virus packages ~45% wild-type RNA genome levels and the quantities of reverse transcription intermediates is 3 to 5% that of wild-type virus. The reduction in reverse transcription intermediates correlates with the results obtained from the HCLZ infectivity analysis (Fig. 3A). The reduction in reverse transcription intermediates is similar for all of the target sequences analyzed, suggesting that there may be an initiation defect or a defect in $tRNA^{Lys,3}$ primer placement. Thus, once reverse transcription starts, it is able to proceed normally. In addition, a reduction in the level of $tRNA^{Lys,3}$ primer on the primer binding site of the genomic RNA would account for the overall observed reduction in reverse transcription in cells infected with the CNBP-5 mutant.

The protein processing and RNA packaging defects may account for some of the reduction in replication and infectivity. Other reasons why CNBP-5 is defective may have to do with the following points: (i) CNBP-5 has only one basic residue, whereas all other HIV-1 and CNBP Zn^{2+} fingers have at least two; (ii) there is a Ser residue after the aromatic amino acid in loop 1—all others have Arg, Asn, or Lys residues at this position; and (iii) CNBP-5 is the only Zn^{2+} finger with a net negative 2 charge, whereas all other Zn^{2+} fingers have a −1, 0, or +1 charge. Additionally, the HODAP procedure shows limitations of conformations that the CNBP-5 Zn^{2+} finger can adopt, which can be accommodated in CNBP-3 and the NH_2-terminal HIV-1 NC Zn^{2+} finger (Fig. 4). Intercalation of the aromatic Trp residue between nucleic acid bases during binding of NC to RNA has been demonstrated with the COOH-terminal NC Zn^{2+} finger (37); presumably, the aromatic residue in the NH_2-terminal finger of HIV-1 NC participates in a similar interaction. Thus, the limited conformations that the CNBP-5 Zn^{2+} finger can adopt may prevent proper intercalations from taking place. This may decrease the binding affinity of CNBP-5 NC to the genomic RNA Ψ site, explaining the reduction in full-length genomic RNA levels in the mutant

viruses. In addition, DeGuzman et al. (13) have shown that Phe-2 and Ile-10, along with Ala-11 in the wild-type Zn^{2+} finger, interact with a hydrophobic cleft in the loop of SL3, which may be disrupted by the aberrant interactions that take place in CNBP-5. This may also account for the defects seen in RNA packaging in the CNBP-5 NC mutant.

The HODAP technique employed in the present study permits the comparison of critical features within a set of Zn^{2+} finger peptides. Because the method accounts for every atom-atom interaction and because it is distance dependent, the interaction data contains a spatial component. Analysis of sequence data alone does not yield three-dimensional spatial information. Similarly, the analysis of three-dimensional atom positions without interaction information does not yield chemical information. The HINT function included in this analysis supplements the spatial component of the data with entropic interaction information. Critical features in Zn^{2+} finger peptides are revealed by using the methods employed here because the features are dynamic physicochemical phenomena with a spatial component. Furthermore, because the essentials of these trajectory motions are viewed through the hydropathic, entropic lens provided by these techniques, a more complete picture of protein design emerges.

The critical and central requirement for NC and the Zn^{2+} fingers in the replication of retroviruses makes them attractive targets for antiviral therapies. However, the results of the present study indicate a need for some caution. For the most part, Zn^{2+} fingers from CNBP are suitable substitutes for the NH_2-terminal NC Zn^{2+} finger of HIV-1. It is remotely possible that mutations in genes coding for NC Zn^{2+} fingers could be complemented by genes that encode cellular (CNBP) Zn^{2+} fingers. Thus, NC mutant DNA vaccines such as those described previously (21) would have to be engineered so that lesions are introduced in other regions in addition to those in the NC-coding region. Additionally, antiviral compounds specific to NC Zn^{2+} fingers may affect CNBP and related proteins; therefore, precautions must be employed during their development so as not to disrupt any critical cellular functions provided by these Zn^{2+} finger-containing proteins.

ACKNOWLEDGMENTS

The Advanced Biomedical Computing Center of the National Cancer Institute at Frederick kindly provided computational resources, including computer time and software licenses.

This work has been funded in whole or in part with Federal funds from the National Cancer Institute, National Institutes of Health, under contract NO1-CO-12400 with SAIC—Frederick, Inc.

The contents of this publication do not necessarily reflect the views or policies of the Department of Health and Human Services, nor does mention of trade names, commercial products, or organization imply endorsement by the U.S. Government.

REFERENCES

1. **Adachi, A., H. E. Gendelman, S. Koenig, T. Folks, R. Willey, A. Rabson, and M. A. Martin.** 1986. Production of acquired immunodeficiency syndrome-associated retrovirus in human and nonhuman cells transfected with an infectious molecular clone. J. Virol. **59:**284–291.
2. **Anderson, C. Y., G. E. Kellogg, and R. J. Freer.** 1997. C5aR ligand peptide 3D QSAR study performed with an applied linear conformation. J. Peptide Res. **49:**476–483.
3. **Armas, P., M. O. Cabada, and N. B. Calcaterra.** 2001. Primary structure and developmental expression of *Bufo arenarum* cellular nucleic acid-binding protein: changes in subcellular localization during early embryogenesis. Dev. Growth Differ. **43:**13–23.
4. **Berg, J. M.** 1986. Potential metal-binding domains in nucleic acid binding proteins. Science **232:**485–487.
5. **Berkowitz, R., J. Fisher, and S. P. Goff.** 1996. RNA packaging. Curr. Top. Microbiol. Immunol. **214:**177–218.
6. **Briggs, M. R., C. Yokoyama, X. Wang, M. S. Brown, and J. L. Goldstein.** 1993. Nuclear protein that binds sterol regulatory element of low density lipoprotein receptor promoter. I. Identification of the protein and delineation of its target nucleotide sequence. J. Biol. Chem. **268:**14490–14496.
7. **Buckman, J. S., W. J. Bosche, and R. J. Gorelick.** 2003. Human immunodeficiency virus-type 1 nucleocapsid Zn^{2+} fingers are required for efficient reverse transcription, initial integration processes, and protection of newly synthesized viral DNA. J. Virol. **77:**1469–1480.
8. **Carteau, S., S. C. Batson, L. Poljak, J. F. Mouscadet, H. de Rocquigny, J. L. Darlix, B. P. Roques, E. Kas, and C. Auclair.** 1997. Human immunodeficiency virus type 1 nucleocapsid protein specifically stimulates Mg^{2+}-dependent DNA integration in vitro. J. Virol. **71:**6225–6229.
9. **Carteau, S., R. J. Gorelick, and F. D. Bushman.** 1999. Coupled integration of human immunodeficiency virus type 1 cDNA ends by purified integrase in vitro: stimulation by the viral nucleocapsid protein. J. Virol. **73:**6670–6679.
10. **Cimarelli, A., S. Sandin, S. Hoglund, and J. Luban.** 2000. Basic residues in human immunodeficiency virus type 1 nucleocapsid promote virion assembly via interaction with RNA. J. Virol. **74:**3046–3057.
11. **Covey, S. N.** 1986. Amino acid sequence homology in gag region of reverse transcribing elements and the coat protein gene of cauliflower mosaic virus. Nucleic Acids Res. **14:**623–633.
12. **De Dominicis, A., F. Lotti, P. Pierandrei-Amaldi, and B. Cardinali.** 2000. cDNA cloning and developmental expression of cellular nucleic acid-binding protein (CNBP) gene in *Xenopus laevis*. Gene **241:**35–43.
13. **DeGuzman, R. N., Z. R. Wu, C. C. Stalling, L. Pappalardo, P. N. Borer, and M. F. Summers.** 1998. Structure of the HIV-1 nucleocapsid protein bound to the SL3 psi-RNA recognition element. Science **279:**384–388.
14. **Dorfman, T., J. Luban, S. P. Goff, W. A. Haseltine, and H. G. Gottlinger.** 1993. Mapping of functionally important residues of a cysteine-histidine box in the human immunodeficiency virus type 1 nucleocapsid protein. J. Virol. **67:**6159–6169.
15. **Feng, Y. X., T. D. Copeland, L. E. Henderson, R. J. Gorelick, W. J. Bosche, J. G. Levin, and A. Rein.** 1996. HIV-1 nucleocapsid protein induces "maturation" of dimeric retroviral RNA in vitro. Proc. Natl. Acad. Sci. USA **93:**7577–7581.
16. **Fisher, R. J., A. Rein, M. Fivash, M. A. Urbaneja, J. R. Casas-Finet, M. Medaglia, and L. E. Henderson.** 1998. Sequence-specific binding of human immunodeficiency virus type 1 nucleocapsid protein to short oligonucleotides. J. Virol. **72:**1902–1909.
17. **Freed, E. O.** 1998. HIV-1 gag proteins: diverse functions in the virus life cycle. Virology **251:**1–15.
18. **Fu, W., R. J. Gorelick, and A. Rein.** 1994. Characterization of human immunodeficiency virus type 1 dimeric RNA from wild-type and protease-defective virions. J. Virol. **68:**5013–5018.
19. **Fu, W., and A. Rein.** 1993. Maturation of dimeric viral RNA of Moloney murine leukemia virus. J. Virol. **67:**5443–5449.
20. **Gorelick, R. J., R. E. Benveniste, T. D. Gagliardi, T. A. Wiltrout, L. K. Busch, W. J. Bosche, L. V. Coren, J. D. Lifson, P. J. Bradley, L. E. Henderson, and L. O. Arthur.** 1999. Nucleocapsid protein zinc finger mutants of simian immunodeficiency virus strain mne produce virions that are replication defective in vitro and in vivo. Virology **253:**259–270.
21. **Gorelick, R. J., R. E. Benveniste, J. D. Lifson, J. L. Yovandich, W. R. Morton, L. Kuller, B. M. Flynn, B. A. Fisher, J. L. Rossio, M. Piatak, Jr., J. W. Bess, Jr., L. E. Henderson, and L. O. Arthur.** 1949. 2000. Protection of *Macaca nemestrina* from disease following pathogenic simian immunodeficiency virus (SIV) challenge: utilization of SIV nucleocapsid mutant DNA vaccines with or without an SIV protein boost. J. Virol. **74:**11935–11941.
22. **Gorelick, R. J., D. J. Chabot, D. E. Ott, T. D. Gagliardi, A. Rein, L. E. Henderson, and L. O. Arthur.** 1996. Genetic analysis of the zinc finger in the Moloney murine leukemia virus nucleocapsid domain: replacement of zinc-coordinating residues with other zinc-coordinating residues yields noninfectious particles containing genomic RNA. J. Virol. **70:**2593–2597.
23. **Gorelick, R. J., D. J. Chabot, A. Rein, L. E. Henderson, and L. O. Arthur.** 1993. The two zinc fingers in the human immunodeficiency virus type 1 nucleocapsid protein are not functionally equivalent. J. Virol. **67:**4027–4036.
24. **Gorelick, R. J., W. Fu, T. D. Gagliardi, W. J. Bosche, A. Rein, L. E. Henderson, and L. O. Arthur.** 1999. Characterization of the block in replication of nucleocapsid protein zinc finger mutants from Moloney murine leukemia virus. J. Virol. **73:**8185–8195.
25. **Gorelick, R. J., T. D. Gagliardi, W. J. Bosche, T. A. Wiltrout, L. V. Coren, D. J. Chabot, J. D. Lifson, L. E. Henderson, and L. O. Arthur.** 1999. Strict conservation of the retroviral nucleocapsid protein zinc finger is strongly influenced by its role in viral infection processes: characterization of HIV-1 particles containing mutant nucleocapsid zinc-coordinating sequences. Virology **256:**92–104.
26. **Gorelick, R. J., L. E. Henderson, J. P. Hanser, and A. Rein.** 1988. Point mutants of Moloney murine leukemia virus that fail to package viral RNA:

evidence for specific RNA recognition by a "zinc finger-like" protein sequence. Proc. Natl. Acad. Sci. USA **85:**8420–8424.
27. **Gorelick, R. J., S. M. Nigida, Jr., J. W. Bess, Jr., L. O. Arthur, L. E. Henderson, and A. Rein.** 1990. Noninfectious human immunodeficiency virus type 1 mutants deficient in genomic RNA. J. Virol. **64:**3207–3211.
28. **Gussio, R., N. Pattabiraman, G. E. Kellogg, and D. W. Zaharevitz.** 1998. Use of 3D QSAR methodology for data mining the National Cancer Institute Repository of Small Molecules: application to HIV-1 reverse transcriptase inhibition. Methods **14:**255–263.
29. **Gussio, R., N. Pattabiraman, D. W. Zaharevitz, G. E. Kellogg, I. A. Topol, W. G. Rice, C. A. Schaeffer, J. W. Erickson, and S. K. Burt.** 1996. All-atom models for the non-nucleoside binding site of HIV-1 reverse transcriptase complexed with inhibitors: a 3D QSAR approach. J. Med. Chem. **39:**1645–1650.
30. **Hendrickson, A. E., and P. O. White.** 1964. Promax: a quick method for rotation to oblique simple structure. Br. J. Psychol. Stat. Sect. **3:**159–165.
31. **Kellogg, G. E., and D. J. Abraham.** 1992. KEY, LOCK, and LOCKSMITH: complementary hydropathic map predictions of drug structure from a known receptor-receptor structure from known drugs. J. Mol. Graph. **10:**212–226.
32. **Kellogg, G. E., L. B. Kier, P. Gaillard, and L. H. Hall.** 1996. E-state fields: applications to 3D QSAR. J. Comput. Aided Mol. Des. **10:**513–520.
33. **Kellogg, G. E., J. N. Scarsdale, and F. A. Fornari, Jr.** 1998. Identification and hydropathic characterization of structural features affecting sequence specificity for doxorubicin intercalation into DNA double-stranded polynucleotides. Nucleic Acids Res. **26:**4721–4732.
34. **Kellogg, G. E., S. F. Semus, and D. J. Abraham.** 1991. HINT: a new method of empirical hydrophobic field calculation for CoMFA. J. Comput. Aided Mol. Des. **5:**545–552.
35. **Konicek, B. W., X. Xia, T. Rajavashisth, and M. A. Harrington.** 1998. Regulation of mouse colony-stimulating factor-1 gene promoter activity by AP1 and cellular nucleic acid-binding protein. DNA Cell Biol. **17:**799–809.
36. **Krizek, B. A., D. L. Merkle, and J. M. Berg.** 1993. Ligand variation and metal ion binding specificity in zinc finger peptides. Inorg. Chem. **32:**937–940.
37. **Lam, W. C., A. H. Maki, J. R. Casas-Finet, J. W. Erickson, B. P. Kane, R. C. Sowder II, and L. E. Henderson.** 1994. Phosphorescence and optically detected magnetic resonance investigation of the binding of the nucleocapsid protein of the human immunodeficiency virus type 1 and related peptides to RNA. Biochemistry **33:**10693–10700.
38. **Lay, D. C.** 1994. Linear algebra and its applications. Addison-Wesley, New York, N.Y.
39. **Liu, M., K. U. Kumar, M. M. Pater, and A. Pater.** 1998. Identification and characterization of a JC virus pentanucleotide repeat element binding protein: cellular nucleic acid binding protein. Virus Res. **58:**73–82.
40. **Meng, E. C., I. D. Kuntz, D. J. Abraham, and G. E. Kellogg.** 1994. Evaluating docked complexes with the HINT exponential function and empirical atomic hydrophobicities. J. Comput. Aided Mol. Des. **8:**299–306.
41. **Ness, G. C., R. K. Keller, and L. C. Pendleton.** 1991. Feedback regulation of hepatic 3-hydroxy-3-methylglutaryl-CoA reductase activity by dietary cholesterol is not due to altered mRNA levels. J. Biol. Chem. **266:**14854–14857.
42. **Osborne, T. F., G. Gil, J. L. Goldstein, and M. S. Brown.** 1988. Operator constitutive mutation of 3-hydroxy-3-methylglutaryl coenzyme A reductase promoter abolishes protein binding to sterol regulatory element. J. Biol. Chem. **263:**3380–3387.
43. **Pellizzoni, L., F. Lotti, S. A. Rutjes, and P. Pierandrei-Amaldi.** 1998. Involvement of the *Xenopus laevis* Ro60 autoantigen in the alternative interaction of La and CNBP proteins with the 5′UTR of L4 ribosomal protein mRNA. J. Mol. Biol. **281:**593–608.
44. **Popovic, M., M. G. Sarngadharan, E. Read, and R. C. Gallo.** 1984. Detection, isolation, and continuous production of cytopathic retroviruses (HTLV-III) from patients with AIDS and pre-AIDS. Science **224:**497–500.
45. **Rajavashisth, T. B., A. K. Taylor, A. Andalibi, K. L. Svenson, and A. J. Lusis.** 1989. Identification of a zinc finger protein that binds to the sterol regulatory element. Science **245:**640–643.
46. **Rein, A., L. E. Henderson, and J. G. Levin.** 1998. Nucleic-acid-chaperone activity of retroviral nucleocapsid proteins: significance for viral replication. Trends Biochem. Sci. **23:**297–301.
47. **Ruble, D. M., and D. N. Foster.** 1998. Molecular cloning and characterization of a highly conserved chicken cellular nucleic acid binding protein cDNA. Gene **218:**95–101.
48. **Rummel, R. J.** 1970. Applied factor analysis. Northwestern University Press, Evanston, Ill.
49. **Shen, N., L. Jette, C. Liang, M. A. Wainberg, and M. Laughrea.** 2000. Impact of human immunodeficiency virus type 1 RNA dimerization on viral infectivity and of stem-loop B on RNA dimerization and reverse transcription and dissociation of dimerization from packaging. J. Virol. **74:**5729–5735.
50. **Summers, M. F., L. E. Henderson, M. R. Chance, J. W. Bess, Jr., T. L. South, P. R. Blake, I. Sagi, G. Perez-Alvarado, R. C. Sowder III, D. R. Hare, and L. O. Arthur.** 1992. Nucleocapsid zinc fingers detected in retroviruses: EXAFS studies of intact viruses and the solution-state structure of the nucleocapsid protein from HIV-1. Protein Sci. **1:**563–574.
51. **Tanchou, V., D. Decimo, C. Pechoux, D. Lener, V. Rogemond, L. Berthoux, M. Ottmann, and J. L. Darlix.** 1998. Role of the N-terminal zinc finger of human immunodeficiency virus type 1 nucleocapsid protein in virus structure and replication. J. Virol. **72:**4442–4447.
52. **van Regenmortel, M. H. V., C. M. Fauquet, D. H. L. Bishop, E. B. Carstens, M. K. Estes, S. M. Lemon, J. Maniloff, M. A. Mayo, D. J. McGeoch, C. R. Pringle, and R. B. Wickner.** 2000. Virus taxonomy: classification and nomenclature of viruses. Seventh report of the International Committee on Taxonomy of Viruses. Academic Press, San Diego, Calif.
53. **Vo, T. A., M. Minet, J. M. Schmitter, F. Lacroute, and F. Wyers.** 2001. Mpe1, a zinc knuckle protein, is an essential component of yeast cleavage and polyadenylation factor required for the cleavage and polyadenylation of mRNA. Mol. Cell. Biol. **21:**8346–8356.
54. **Wang, X., M. R. Briggs, X. Hua, C. Yokoyama, J. L. Goldstein, and M. S. Brown.** 1993. Nuclear protein that binds sterol regulatory element of low density lipoprotein receptor promoter. II. Purification and characterization. J. Biol. Chem. **268:**14497–14504.
55. **Warden, C. H., S. K. Krisans, D. Purcell-Huynh, L. M. Leete, A. Daluiski, A. Diep, B. A. Taylor, and A. J. Lusis.** 1994. Mouse cellular nucleic acid binding proteins: a highly conserved family identified by genetic mapping and sequencing. Genomics **24:**14–19.
56. **Yokoyama, C., X. Wang, M. R. Briggs, A. Admon, J. Wu, X. Hua, J. L. Goldstein, and M. S. Brown.** 1993. SREBP-1, a basic-helix-loop-helix-leucine zipper protein that controls transcription of the low density lipoprotein receptor gene. Cell **75:**187–197.